





Article

# Multi-Disciplinary Optimisation of Road Vehicle Chassis Subsystems <sup>†</sup>

Liunan Yang <sup>1,2,3</sup> , Massimiliano Gobbi <sup>1,\*</sup> , Gianpiero Mastinu <sup>1</sup>, Giorgio Previati <sup>1</sup>  and Federico Ballo <sup>1</sup> 

<sup>1</sup> Department of Mechanical Engineering, Politecnico di Milano, 20156 Milan, Italy; liunan.yang@polimi.it (L.Y.); gianpiero.mastinu@polimi.it (G.M.); giorgio.previati@polimi.it (G.P.); federicomaria.ballo@polimi.it (F.B.)

<sup>2</sup> Chongqing Changan Automobile Company, Chongqing 401120, China

<sup>3</sup> College of Mechanical and Vehicle Engineering, Chongqing University, Chongqing 400044, China

\* Correspondence: massimiliano.gobbi@polimi.it

<sup>†</sup> This paper is an extended version of the work presented by the same authors at the ASME 2019 International Design Engineering Technical Conferences, Anaheim, CA, USA, 18–21 August, 2019; Paper no.: DETC2019-97308.

**Abstract:** Two vehicle chassis design tasks were solved by decomposition-based multi-disciplinary optimisation (MDO) methods, namely collaborative optimisation (CO) and analytical target cascading (ATC). A passive suspension system was optimised by applying both CO and ATC. Multiple parameters of the spring and damper were selected as design variables. The discomfort, road holding, and total mass of the spring–damper combination were the objective functions. An electric vehicle (EV) powertrain design problem was considered as the second test case. Energy consumption and gradeability were optimised by including the design of the electric motor and the battery pack layout. The standard single-level all-in-one (AiO) multi-objective optimisation method was compared with ATC and CO methods. AiO methods showed some limitations in terms of efficiency and accuracy. ATC proved to be the best choice for the design problems presented in this paper, since it provided solutions with good accuracy in a very efficient way. The proposed investigation on MDO methods can be useful for designers, to choose the proper optimisation approach, while solving complex vehicle design problems.

**Keywords:** multi-disciplinary optimisation; analytical target cascading; collaborative optimisation; passive suspension; electric vehicle powertrain



**Citation:** Yang, L.; Gobbi, M.; Mastinu, G.; Previati, G.; Ballo, F. Multi-Disciplinary Optimisation of Road Vehicle Chassis Subsystems. *Energies* **2022**, *15*, 2172. <https://doi.org/10.3390/en15062172>

Academic Editor: Pablo García-Triviño and Carlos Andrés García-Vázquez

Received: 7 February 2022

Accepted: 11 March 2022

Published: 16 March 2022

**Publisher's Note:** MDPI stays neutral with regard to jurisdictional claims in published maps and institutional affiliations.



**Copyright:** © 2022 by the authors. Licensee MDPI, Basel, Switzerland. This article is an open access article distributed under the terms and conditions of the Creative Commons Attribution (CC BY) license (<https://creativecommons.org/licenses/by/4.0/>).

## 1. Introduction

In the automotive field, multi-disciplinary design problems typically involve several groups of experts. They are responsible for different performances and for designing different subsystems that constitute the vehicle. The expert groups must interact during the development process. Some groups are responsible for the design (e.g., the body, the powertrain, the suspension system, etc.), while other groups are responsible for different performance metrics (e.g., handling, safety, noise, vibration, and harshness (NVH), etc.). Traditionally, the design process and the assessment of performance are divided into parallel phases with intermediate synchronisation phases (usually “design review meeting”) between the groups.

Although the traditional approach leads to a feasible design, it may not be the optimal choice. The purpose of MDO is to obtain the optimal solution by taking several disciplines into account simultaneously. In this way, the design groups can work in parallel and autonomously [1,2]. The most common optimisation approach to handle the computationally demanding simulation models involves the use of metamodels [1,3]. Metamodels need to be created by the design groups before the optimisation process, and they offer an easy way of distributing the design work. The single-level optimisation method, AiO, in combination with metamodels, is the most straightforward way of implementing multi-disciplinary

methods in the development of automotive subsystems. Complex projects can be deployed into small sub-problems rather than applying the AiO approach. A problem can be decomposed in different ways. Discipline-based decomposition refers to dividing the problem on the basis of the different disciplines. In this case, the decomposition consists of two levels, one top level and one for all disciplines.

Subsystem-based decomposition refers to dividing the system into its constituent subsystems, which can be further subdivided into components. In this case, an arbitrary number of levels is obtained. By using multi-level optimisation techniques, the problem can be decomposed into multiple manageable sub-problems, and the interactions between them can be managed using coordination strategies, such as CO, ATC, bi-level integrated system synthesis (BLISS), and concurrent subspace optimisation (CSSO). The ATC method [4] is the most common MDO method applied in the vehicle development process, such as suspensions design [5,6], heavy truck design [7], engine calibration [8], optimisation of hybrid electric powertrains [9], continuously variable transmission design [10], and passive safety optimisation [11]. The convergence of the method was proved in [12]. The CO was developed for aerospace optimisation problem [13,14], and applications to vehicle development are limited to the body structure design [15,16]. A comparison between ATC and CO can be found in [17]. The robustness of CO can be a disadvantage since it has shown instabilities at convergence [18]. Other MDO methods can be applied to solve vehicle design problems as well [19–22].

In this paper, two problems with different levels of complexity are solved by MDO methods. The first problem is the optimisation of the suspension system performance by including the geometry of spring and damper as design variables. Another problem is the optimisation of the performance of EV powertrain by including the design of the battery pack and the electric motors. CO and ATC, as well as the conventional AiO methods, are analysed and compared.

## 2. Suspension Optimisation

The suspension system is closely related to ride quality and active safety of the vehicle. The vertical dynamics of the vehicle with conventional passive suspension was well studied by using the simplified quarter-car model of Figure 1 [23–30]. The optimal suspension setting always involves a compromise among multiple performance indices by designing spring and damping settings [6,31]. However, the spring stiffness and damping coefficient are related to the actual design of the spring and damper. The damper is fitted inside the spring coils in most of the front suspensions and some rear suspensions. Thus, it is more practical to consider the geometry of the spring and damper as design variables, with constraints related to the assembly requirements [32]. The mass of the spring and damper was minimised to converge to an engineering relevant solution, considering the same spring stiffness and damping coefficient levels can be obtained by different sets of dimensions.

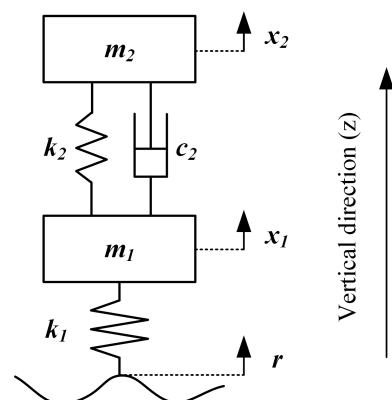


Figure 1. Quarter-car model, adapted from [2].

### 2.1. Optimisation Problem Definition

In the quarter-car model utilised to analyse the vertical dynamics (Figure 1),  $m_1$  and  $m_2$  represent the unsprung mass and sprung mass, respectively,  $x_1$  and  $x_2$  are the corresponding vertical displacements.  $k_1$  represents the radial stiffness of the tyre.  $k_2$  and  $c_2$  represent the spring stiffness and damping coefficient. A single slope PSD defined by vehicle speed  $v$  and road profile parameter  $A_b$  represents road excitation  $r$  [31]. A typical compact car is considered as the reference vehicle in the following analysis. The data of the quarter-car model and running conditions are listed in Table 1 [33].

**Table 1.** Data of the quarter-car model and vehicle running conditions.

Parameters	Meaning	Value	Unit
$m_1$	Unsprung mass	31	kg
$m_2$	Sprung mass	229	kg
$k_1$	Tyre radial stiffness	120,000	N/m
$v$	Vehicle speed	30	m/s
$A_b$	Road profile parameter	$1.4 \times 10^{-5}$	m

The spring and damper settings were properly designed to obtain optimal suspension performance, namely discomfort ( $\sigma_{\ddot{x}_2}$ ) and road holding ( $\sigma_{F_z}$ ). Discomfort is defined as the standard deviation of vehicle body vertical acceleration; road holding is defined as the standard deviation of dynamic tyre load. These two performance indices and the total mass of spring and damper ( $m_{k2} + m_{c2}$ ) are considered as objective functions.

The sketch of the spring and damper is shown in Figure 2, in which the main dimensions are labelled. The selected design variables and their bounds are listed in Table 2.

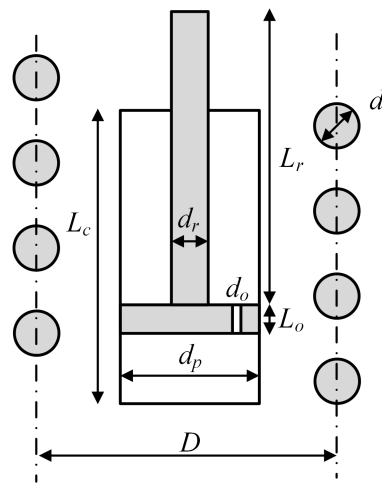


**Figure 2.** Sketch of the spring and damper.

**Table 2.** Design variables for the suspension optimisation problem.

Variables	Meaning	Lower Bound	Upper Bound	Unit d
$i_c$	Number of spring coils	4	10	
$D$	Spring diameter	100	200	mm
$d$	Wire diameter	5	15	mm
$d_r$	Rod diameter	8	25	mm
$d_o$	Orifice diameter	1	5	mm
$d_p$	Piston diameter	40	60	mm

Other geometrical dimensions of the damper are assumed as constant parameters, listed in Table 3.

**Table 3.** Constant parameters of the damper.

Parameters	Meaning	Value	Unit
$L_c$	Length of cylinder	250	mm
$L_r$	Length of rod	300	mm
$L_o$	Length of orifice	10	mm

The spring stiffness and damping coefficient can be related to their geometry as

$$k_2 = \frac{Gd^4}{8D^3i_c} \quad (1)$$

$$c_2 = \frac{32L_o\mu}{d_o^2} \frac{(A_p - A_r)^2}{A_o} \quad (2)$$

Since the spring is usually made of steel, the shear modulus  $G$  is assumed to be  $79,300 \times 10^6$  Pa. The dynamic viscosity  $\mu$  of the fluid in the damper is 0.04 Pa s.  $A_r$ ,  $A_o$ ,  $A_p$  are the area of the rod, orifice, and piston, computed as

$$\begin{aligned} A_r &= \frac{\pi d_r^2}{4} \\ A_o &= \frac{\pi d_o^2}{4} \\ A_p &= \frac{\pi d_p^2}{4} \end{aligned} \quad (3)$$

The expressions of discomfort and road holdings can be derived as functions of the spring stiffness  $k_2$  and damping coefficient  $c_2$  [31,34]. They are reported in Equations (4) and (5), respectively.

- Discomfort

$$\sigma_{\ddot{x}_2} = \sqrt{A_b v \frac{k_1 c_2^2 + (m_1 + m_2) k_2^2}{2c_2 m_2^2}} \quad (4)$$

- Road holding

$$\sigma_{F_z} = \sqrt{A_b v (b_1 c_2 + b_2 c_2^{-1})} \quad (5)$$

where

$$\begin{aligned} b_1 &= \frac{(m_1 + m_2)^2 k_1}{2m_2^2} \\ b_2 &= \frac{(m_1 + m_2)^3 k_2^2 - 2m_1 m_2 (m_1 + m_2) k_1 k_2 + m_1 (m_2 k_1)^2}{2m_2^2} \end{aligned} \quad (6)$$

By substituting Equations (1) and (2) into Equations (4) and (5), discomfort and road holding can be rewritten as functions of the variables in Table 2.

- Spring mass

$$m_{k2} = \frac{\pi^2 d^2 D i_c}{4} \rho \quad (7)$$

where  $\rho = 7850$  kg/m<sup>3</sup> (steel).

- Damper mass

$$m_{c2} = \left( \frac{\pi d_p^2}{4} L_o - \frac{\pi d_o^2}{4} L_o + \frac{\pi d_r^2}{4} L_r + \pi \left( \left( \frac{d_p}{2} + 0.002 \right)^2 - \left( \frac{d_p}{2} \right)^2 \right) L_c \right) \rho + m_{oil} \quad (8)$$

where  $\rho = 7850$  kg/m<sup>3</sup> (steel).

The oil mass  $m_{oil}$  in the damper is 0.3 kg, the piston height is the same as the orifice length  $L_o$ , the thickness of the damper tube is 0.002 m.

The constraints are defined based on structural integrity and geometric limitations of the components.

The explanation of the design constraints is presented in Table 4. The structural integrity of the spring has to be guaranteed; therefore, the maximum stress  $\tau_{max}$  has to be lower than the material admissible stress  $\tau_{adm}$

$$\tau_{max} \leq \tau_{adm} \quad (9)$$

**Table 4.** Design constraints for the suspension optimisation problem.

Constraints	Meaning
$g_1$	Maximum shear stress of the spring material $\leq$ admissible shear stress
$g_2$	Maximum spring deflection (maximum compression) $\leq$ admissible spring deflection
$g_3$	Geometry constraint, the damper is placed inside the helical spring
$g_4$	Damper geometry constraint

The material admissible shear stress  $\tau_{adm}$  is 1100 MPa. The maximum stress  $\tau_{max}$  in Equation (9) depends on the load and spring geometry, it reads

$$\tau_{max} = \frac{8FDW}{\pi d^3} \quad (10)$$

where  $F$  is the spring force when the spring is fully compressed,  $W$  is the Wahl correction factor. Their calculations are given below

$$\begin{aligned} F &= k_2(L_f - L_s) \\ L_s &= (i_c + 1)d \\ W &= \frac{4c-1}{4c-4} + \frac{0.615}{e} \\ e &= \frac{D}{d} \end{aligned} \quad (11)$$

$L_s$  is the spring solid length (assuming a plain ends spring),  $L_f$  is the spring free length (0.3 m), and  $e$  is the spring index.

The maximum compression of the spring is limited by its solid length  $L_s$ . Assuming a target maximum compression  $y_{max}$  of 0.18 m, the constraint reads

$$y_{max} \leq L_f - L_s \quad (12)$$

The remaining constraints are related to the available room and geometrical feasibility of the damper. The damper has to be placed inside the spring coils; this introduces a relation among the geometrical dimensions of the spring and damper in the form of Equation (13)

$$d_p \leq D - d \quad (13)$$

Finally, a constraint on the orifice diameter is required for a feasible solution

$$d_o \leq \frac{(d_p - d_r)}{2} \quad (14)$$

The problem is a typical multi-objective optimisation problem that can be decomposed. In the following, the problem is solved by different multi-disciplinary optimisation methods, namely AiO, CO, and ATC.

## 2.2. AiO Formulation

The AiO is the conventional formulation that solves the optimisation problem without decomposition. This formulation is the easiest to understand and implement, while its efficiency is one of the main concerns. The suspension optimisation problem is formulated as in Equation (15).

$$\begin{aligned}
 & \min (\sigma_{\ddot{x}_2}, \sigma_{F_z}, m_{k2} + m_{c2}) \\
 & \mathbf{x} = [i_c, d, D, d_p, d_r, d_o] \\
 & g_1 = \tau_{\max} - \tau_{adm} \leq 0 \\
 & g_2 = y_{\max} - (L_f - L_s) \leq 0 \\
 & g_3 = d_p - (D - d) \leq 0 \\
 & g_4 = d_o - \frac{(d_p - d_r)}{2} \leq 0
 \end{aligned} \tag{15}$$

The problem is solved by applying the constraints method. The discomfort ( $\sigma_{\ddot{x}_2}$ ) and total mass ( $m_{k2} + m_{c2}$ ) are converted into two constraints. The road holding ( $\sigma_{F_z}$ ) is minimised at each feasible combination of discomfort and total mass by using a sequential quadratic programming (SQP) algorithm. Proper settings for the SQP algorithm need to be selected in order to obtain accurate solutions efficiently. Tight tolerances are required to obtain accurate solutions, but they may also lead to a large number of iterations or function evaluations, which means lower efficiency. The proper settings are selected by performing a sensitivity analysis of different algorithm parameters, listed in Table 5.

**Table 5.** Settings of optimisation algorithm for the suspension optimisation problem.

Options	Value in AiO	Value in CO	Value in ATC
Algorithm	SQP	interior-point	interior-point
Function Tolerance	$1 \times 10^{-6}$	$1 \times 10^{-10}$	$1 \times 10^{-6}$
Constraints Tolerance	$1 \times 10^{-3}$	$1 \times 10^{-3}$	$1 \times 10^{-6}$
Step Tolerance	$1 \times 10^{-9}$	$1 \times 10^{-6}$	$1 \times 10^{-10}$
Maximum number of iterations allowed	$6 \times 10^4$	$1 \times 10^3$	$1 \times 10^3$
Maximum number of function evaluations allowed	$3 \times 10^6$	$3 \times 10^3$	$3 \times 10^3$

## 2.3. CO Formulation

The CO formulation is shown in Figure 3. Due to the simplicity of the suspension system, the problem was decomposed into a spring subsystem and a damper subsystem based on actual components rather than on disciplines.

All of the objective functions were optimised at the system level with all the design variables, subject to the compatibility constraints ( $g_{01}$  and  $g_{02}$ ). The system level also coordinated with the subsystems by sending and receiving the linking variables. The linking variables included the design variables ( $x$ ) at the system level, which went down as the target to the subsystem level, and the design variables of the subsystems.

The objectives to be minimised in the subsystems were the discrepancies between the values of the design variables at the system level and at the subsystems levels, subjected to the design constraints. In the spring subsystem, the discrepancy of the design variables related to the spring between the system level and subsystems was minimised, considering the dimensions of the spring. The constraints  $g_1$  and  $g_2$  were considered in the spring design. In the damper subsystem, the discrepancy of the design variables related to the damper geometry between the system level and subsystems was minimised. The constraint  $g_4$  is a geometry constraint related to the damper design. The constraint  $g_3$  was a geometry constraint related to both the spring and damper, and it was only considered in the damper subsystem. The optimal solutions of the spring and damper subsystems were sent from the subsystem level to the system level as linking variables.

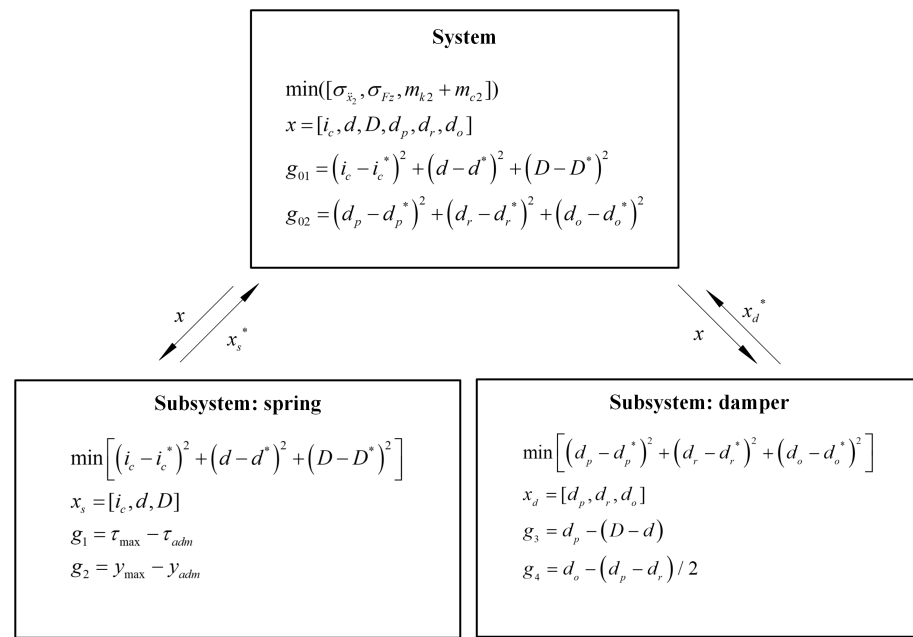


**Figure 3.** CO formulation for the suspension optimisation problem.

The system level was optimised by applying the constraints method, as in the AiO formulation, discomfort ( $\sigma_{\ddot{x}_2}$ ) and total mass ( $m_{k2} + m_{c2}$ ) were converted into two additional constraints. At the first iteration, for a specified maximum level of discomfort and total mass, the road holding ( $\sigma_{F_z}$ ) was optimised and the solution ( $x$ ) was sent to the subsystems as linking variables. Afterwards, the subsystems were optimised by applying the constraints method to minimise the discrepancy between the system design variables ( $x$ ) with respect to the local design variables ( $x_s$  and  $x_d$ ) of the spring and damper subsystems. The local design variables were then sent back to the system level to compute the compatibility constraints ( $g_{01}$  and  $g_{02}$ ) for the next iteration. The termination criterion required that the relative change in the values of the design optimization variables (norm of the difference) after two consecutive CO iterations be smaller than a user-specified small positive threshold (0.01). It should be noted that the design variables should be normalised when calculating the compatibility constraints at the system level and the objective functions at the subsystem level since the order of magnitude of the selected design variables are different.

As in the AiO formulation, the algorithm settings were selected based on a sensitivity analysis. The settings used in the CO formulation are listed in Table 5.

#### 2.4. ATC Formulation

The ATC formulation is described in Figure 4.

Similarly to the CO formulation, the problem was decomposed based on actual components. The objective function total mass ( $m_{k2} + m_{c2}$ ) was divided into spring mass ( $m_{k2}$ ) and damper mass ( $m_{c2}$ ). The system level optimised the vehicle performance discomfort ( $\sigma_{\ddot{x}_2}$ ) and road holding ( $\sigma_{F_z}$ ) considering spring stiffness  $k_2$  and damping coefficient  $c_2$  as design variables. The system level also acted as a coordinator sending the optimal design variables ( $k_2$  and  $c_2$ ) to the subsystems as design targets ( $t_{21}$  and  $t_{22}$ ).

The two subsystems must reach the design targets from the system level. The norm of the discrepancy between the targets ( $t_{21}$  and  $t_{22}$ ) and the responses of the subsystems ( $r_{21}$  and  $r_{22}$ ) were minimised. These target and response variables are called linking variables in ATC formulation since they are the links between the system level and subsystem level. In this problem, the masses of the spring and damper ( $m_{k2}$  and  $m_{r2}$ ) were local objective functions of the subsystems to be optimised.

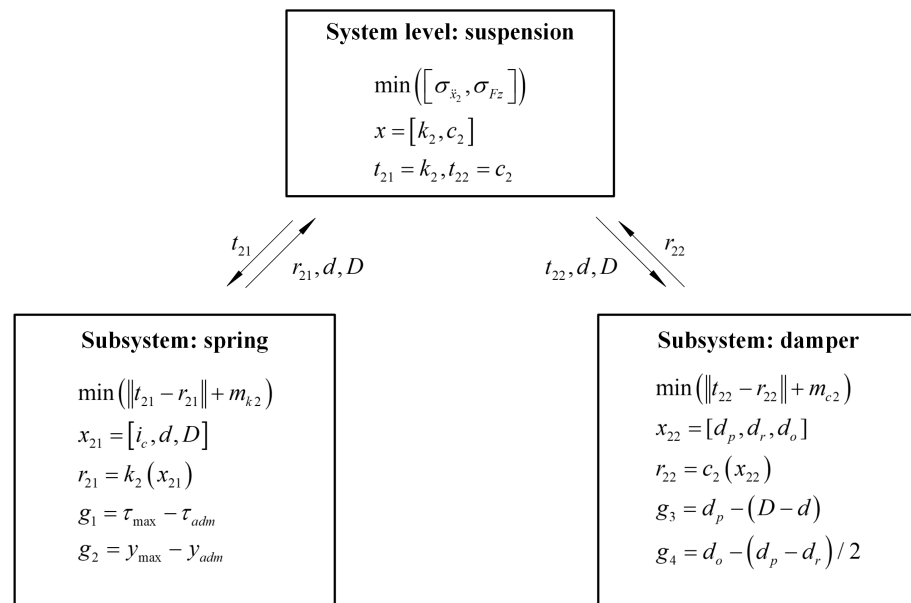


**Figure 4.** ATC formulation for the suspension optimisation problem.

In the spring subsystem, the objective function was the sum of the spring mass and the norm of the target discrepancy ( $m_{k_2} + \|t_{21} - r_{21}\|$ ). The design variables were the three parameters of the spring ( $i_c, d, D$ ), which were a subset of the design variables of the whole optimisation problem. The constraints  $g_1$  and  $g_2$  were related to the spring design.

In the damper subsystem, the objective function was the sum of the damper mass and the norm of the target discrepancy ( $m_{c_2} + \|t_{22} - r_{22}\|$ ). The design variables were related to the geometry of the damper ( $d_p, d_r, d_o$ ), which were the remaining design variables of the whole optimisation problem. The constraint  $g_4$  was a geometry constraint related to the damper design. The constraint  $g_3$  was a geometry constraint related to both the spring and damper, and it was only considered in the damper subsystem. In this case, the design variables  $d$  and  $D$  from the spring subsystem were transferred to the damper subsystem via the system level.  $d$  and  $D$  were called shared variables in the ATC formulation.

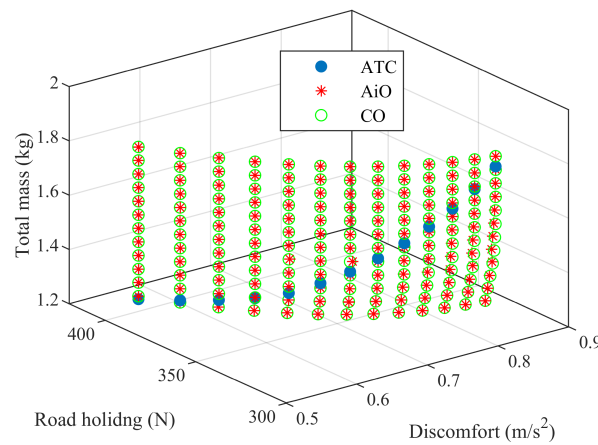
The system level was solved by the constraints method, where the discomfort level (constraint) varied in a predefined range and the road holding was minimised. At each iteration, the system level was optimised and the target spring stiffness and damping coefficient ( $t_{21}$  and  $t_{22}$ ) were sent to the subsystems. Then, the subsystems were optimised to reach the targets and to minimise the masses. At each iteration, the spring subsystem was optimised first, and the shared variables  $d$  and  $D$  were transferred to the damper subsystem. At the end of each iteration, the two subsystems sent the spring stiffness and damping coefficient ( $r_{21}$  and  $r_{22}$ ) back to the system level. The termination criterion required that the relative changes in the values of the normalised design optimization variables (norm of the difference) after two consecutive ATC iterations be smaller than a user-specified small positive threshold (0.01).

As previously done, a sensitivity analysis was performed. The settings used in the ATC formulation were selected considering the best compromise between accuracy and efficiency; they are listed in Table 5.

### 2.5. Solutions and Comparison of the MDO Methods

The optimised solutions of the AiO, CO, and ATC formulations are reported and analysed. The Pareto-optimal sets in the three objective functions domain are shown in Figure 5. For all the formulations, discomfort ranges from 0.55 to 0.85  $m/s^2$ . The total mass in the CO and ATC formulations ranges from 1.25 to 1.8 kg.

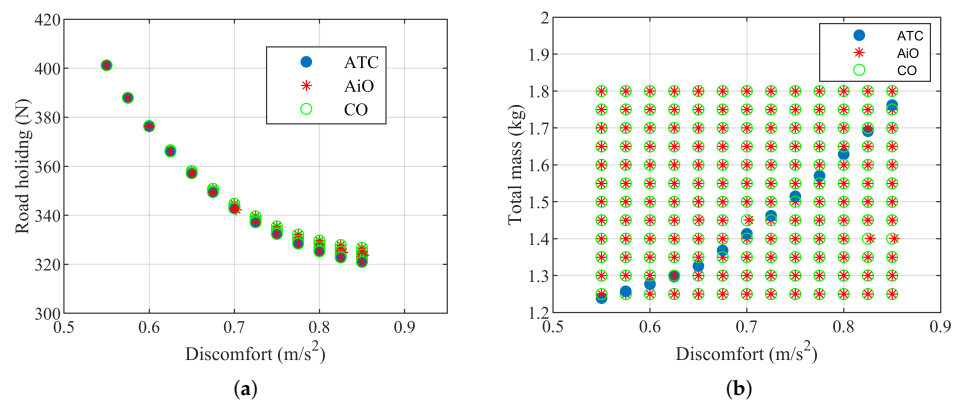




**Figure 5.** Pareto-optimal sets in the objective functions domain.

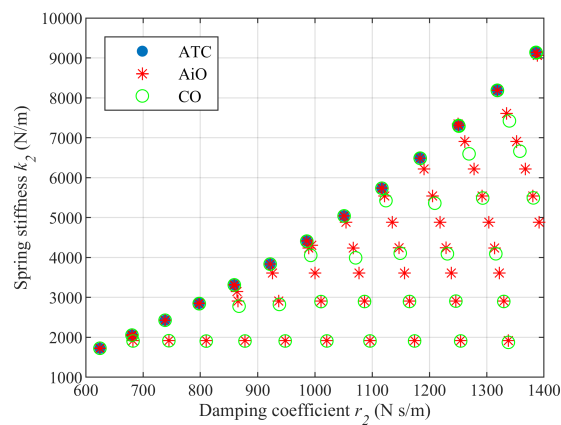
It can be seen that the Pareto-optimal set for ATC is a curve, while the Pareto-optimal sets of AiO and CO form a surface. This is due to the different problem formulations. In AiO, the three objective functions are optimised concurrently. The system level of CO solves the three objective functions in the same way as in the AiO. Therefore, the Pareto-optimal sets for AiO and CO are three-dimensional surfaces. However, in the ATC, discomfort and road holding were optimised first at the system level. Then, the minimum masses were computed in the spring and damper subsystems. Thus, each discomfort level corresponded to one combination of road holding and total mass.

Based on the analysis above, the solutions set for AiO and CO should include the solutions for ATC. The projections of the three-dimensional plot are provided as well for a better understanding of the Pareto-optimal solutions. It can be seen from Figure 6a that the boundaries of AiO and CO solution sets are consistent with the ATC in the discomfort-road holding domain. The solutions in the discomfort-total mass domain are shown in Figure 6b. The discomfort and total mass are the objective functions that were converted to constraints in the AiO and CO.



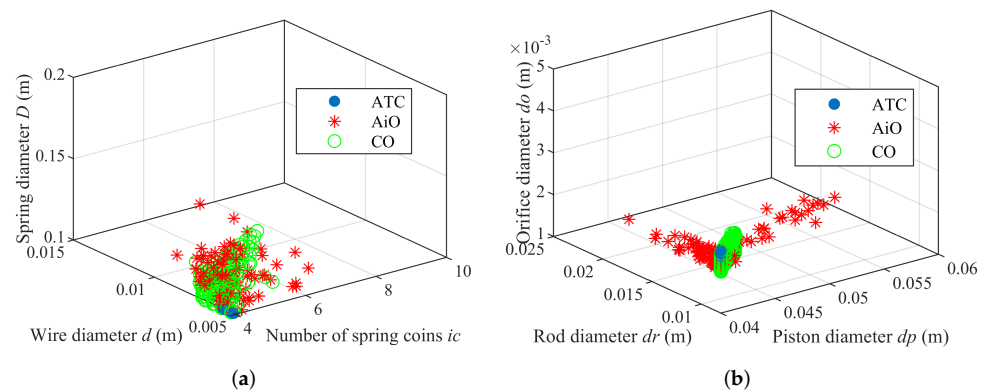
**Figure 6.** Projection of Pareto-optimal sets in the objective functions domain. (a) Projection in discomfort-road holding domain; (b) Projection in discomfort-total mass domain.

Figure 7 shows that the boundaries of AiO and CO solutions match with the ATC in terms of  $k_2$ - $c_2$  domain. The matching solutions of AiO and CO correspond to the solutions that are the closest to the ATC solutions in the objective functions domain.



**Figure 7.** Spring and damper coefficients correspond to the Pareto-optimal sets.

Similarly, some of the AiO and CO solutions match with the ATC in the design variables domain (see Figure 8). The matching solutions for AiO and CO correspond to the solutions that are the closest to the ATC solutions in the objective functions domain. They also correspond to the matching solutions in the  $k_2$ - $c_2$  domain.



**Figure 8.** Pareto-optimal sets in the design variables domain. (a) Results in the wire diameter number of spring coils–spring diameter domain; (b) Results in the piston rod diameter–orifice diameter domain.

According to the formulations and optimal solutions described above, the three formulations were compared by considering transparency, simplicity, efficiency, and accuracy [35]. The comparison of MDO methods on the suspension optimisation problem is provided in Table 6. The term transparency evaluates if the formulation is easy to understand and straightforward in the implementation. Simplicity is also a subjective term, which considers the amount of implementation effort and the complexity to modify the formulation for different optimisation problems. The AiO is the most common formulation. It ranks first in transparency and simplicity. CO and ATC decompose the complex problem into smaller subsystems. The proper linking variables and shared variables need to be selected to connect the system level and subsystems level. In this specific problem, ATC needed to decompose both the objective functions and the constraints, whereas CO only needed to decompose the constraints. Therefore, the CO and ATC were ranked second and third place in both transparency and simplicity.

**Table 6.** Comparison of MDO methods for the suspension optimisation problem.

	Efficiency	Simplicity	Accuracy	Transparency
Best	ATC	AiO	ATC	AiO
↓	CO	CO	AiO	CO
Worst	AiO	ATC	CO	ATC

Efficiency can be evaluated by the number of iterations or the computational time. By applying the constraints method, some objective functions are converted into constraints. The number of iterations and computational effort varies when these objective functions are fixed at different values of the constraints. This is closely related to the initial values of the design variables. An example of computational effort evaluation when discomfort is fixed to  $0.7 \text{ m/s}^2$  is shown in Table 7. Only discomfort is converted into a constraint in ATC, while in AiO and CO, both discomfort and total mass are converted into constraints. The number of iterations refers to the number of calls to the subsystems, so the number of iterations in AiO is always one. The total computational time of the whole optimisation process is the most straightforward metric to evaluate the efficiency. The ranking of the three methods based on efficiency is ATC (8.6 s), CO (220.5 s), and AiO (574.6 s). The ranking remains the same if we compute the computational time per optimal solution. The optimization is performed on a PC with Intel Core i5-8250U CPU and 8 GB RAM.

**Table 7.** Computational effort for the suspension optimisation problem.

Discomfort ( $\text{m/s}^2$ )	ATC Iterations	ATC Time (s)	Mass (kg)	AiO Iterations	AiO Time (s)	CO Iterations	CO Time (s)
0.7	2	1.9525	1.25	1	0.0084	7	1.1663
			1.30	1	0.0073	10	1.3712
			1.35	1	0.0104	10	1.3125
			1.40	1	0.1122	13	1.5624
			1.45	1	0.0180	12	1.0811
			1.50	1	3.2748	15	1.7952
			1.55	1	8.0097	14	1.1449
			1.60	1	13.3667	14	1.2069
			1.65	1	0.0157	13	1.3027
			1.70	1	20.9520	12	1.2134
			1.75	1	0.3253	12	1.1337
1.80	1	0.0166	11	1.2245			

As it can be seen from the Pareto-optimal solutions obtained above, ATC shows the best accuracy (closeness to the actual Pareto-optimal set). AiO and CO consider the three objective functions with the same priority, so the optimal solution set for AiO and CO includes the solutions of ATC. The accuracies of AiO and CO largely depend on the discretisation of the objective functions converted into constraints. AiO with small enough discretisations of the objective functions would provide better accuracy since the levels decoupling in ATC and CO affects the accuracy. Therefore, the ranking of accuracy is ATC, AiO, and CO.

### 3. Electric Vehicle Powertrain Optimisation

Compared with the suspension problem, the EV powertrain problem is significantly more complex. The design of an electric powertrain involves knowledge of the battery, electric motors, and vehicle performance. Therefore, the powertrain design can be decomposed into subsystems based on disciplines and optimised by MDO methods.

The schematic layout of the considered EV is shown in Figure 9. The vehicle equips two in-wheel motors on the rear axle, and the energy is stored in a Li-ion battery pack.

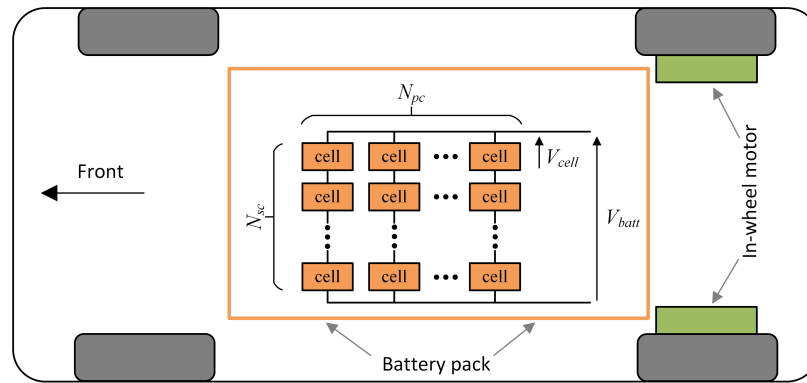


Figure 9. Layout of EV powertrain, adapted from [36].

In this section, AiO, CO, and ATC are considered for the powertrain optimisation problem, to study the performance of MDO methods in a more complex scenario.

### 3.1. Optimisation Problem Definition

The performance of powertrain was evaluated by two conflicting indices, namely energy consumption  $Ec$  and gradeability  $Gr$ . The energy consumption was calculated as the total energy required for running 250 km on the basis of the NEDC. The gradeability was to evaluate the longitudinal performance and tractive ability.

The vehicle specification, battery model, and electric motor model were required to calculate energy consumption and gradeability. The parameters of the EV are provided in Table 8. The  $m_{body}$  includes the vehicle body, the front axle, and two passengers.  $m_{tyre}$  is the mass of a tyre.  $m_{cell}$  is the mass of a single battery cell.  $m_{motorref}$  is the mass of a reference electric motor. The mass of the laden vehicle is

$$m_{vehicle} = m_{body} + 2m_{tyre} + m_{cell}N_{bc} + 2m_{motorref}k_rk_a \quad (16)$$

where the  $N_{bc}$  is the total number of battery cells, the  $k_a$  and  $k_r$  are the scaling factors of the electric motor in axial and radial direction.

Table 8. Electric vehicle parameters.

Parameters	Meaning	Value	Unit
$m_{body}$	Vehicle body mass	800	kg
$m_{tyre}$	Tyre mass	20	kg
$m_{cell}$	Battery cell mass	0.787	kg
$m_{motorref}$	Reference motor mass	30	kg
$N_{EM}$	Number of motors	2	
$R_w$	Wheel radius	0.32	m
$A$	Frontal area	2	m <sup>2</sup>
$C_d$	Coefficient of drag	0.25	
$C_r$	Rolling resistance coefficient	0.01	

- Battery Model

The arrangement of the battery cells is shown in Figure 10.

The total number of battery cells is the product of the number of cells in series  $N_{sc}$  and parallel  $N_{pc}$ .

$$N_{bc} = N_{sc}N_{pc} \quad (17)$$

The rated cell capacity  $C$  is 33.1 Ah, and the average voltage  $V_{cell}$  is 3.8 V. Therefore, the voltage of the battery pack is

$$V_{batt} = N_{sc}V_{cell} \quad (18)$$

The maximum discharge pulse current rate of the Li-ion cell is considered as 3C. So, the current  $I_{batt}$  and output power  $P_{batt}$  of the battery pack are

$$I_{batt} = N_{pc}3C \tag{19}$$

$$P_{batt} = V_{batt}I_{batt} \tag{20}$$

The available energy in the battery pack  $E_{batt}$  is estimated considering 70% of the full capacity in each cell.

$$E_{batt} = 0.7N_{sc}N_{pc}CV_{cell} \tag{21}$$

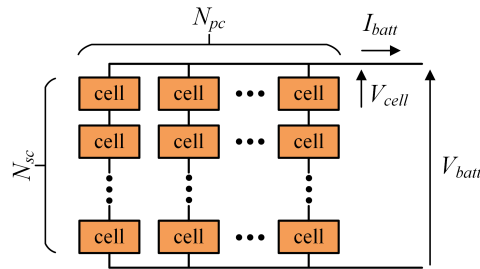


Figure 10. Battery cell layout, adapted from [36].

- Electric Motor Model

The vehicle uses outer rotor surface permanent magnet machines as the in-wheel motors. An analytical motor model built by the relative permeance method described in [37] was selected as the reference model. The reference model can be scaled to estimate the performance, losses, and mass of the actual in-wheel motor. The scaling factors  $k_a$  and  $k_r$  of the motor are described in Figure 11.

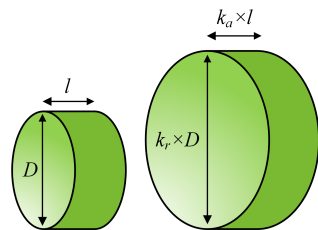


Figure 11. Scaling of the reference motor, adapted from [36,37].

The objective functions gradeability and energy consumption are derived as follows.

### 3.1.1. Gradeability

The gradeability  $Gr$  is the steepness of grade  $\theta$  that a vehicle is able to climb. The calculation of gradeability is given in Equation (22).

$$Gr = \sin(\theta) = \frac{d - C_r^2 \sqrt{1 - d^2 + C_r^2}}{1 + C_r^2} \tag{22}$$

$$d = \left( \frac{T_{peak}\omega_B}{v} - \frac{1}{2}C_d\rho Av^2 \right) \frac{1}{m_{vehicle}g}$$

where frontal area  $A$ , drag coefficient  $C_d$ , and rolling resistance coefficient  $C_r$  are known parameters provided in Table 8. The air density  $\rho$  and vehicle velocity  $v$  are  $1.29 \text{ kg/m}^3$  and  $10 \text{ km/h}$  respectively. The peak torque  $T_{peak}$  is calculated from the motor model.

### 3.1.2. Energy Consumption

The energy consumption  $Ec$  is the energy consumed by the electric motor  $E_{EM}$  and power electronics  $E_{PE}$  within the target range  $R_t$ .

$$E_c = \frac{R_t}{D_{DC}} \frac{N_{EM}(E_{EM} + E_{PE})}{3600 \times 1000} \tag{23}$$

where the range  $R_t$  is 250 km on NEDC.

The  $E_{EM}$  is the integral of the motor input power over the driving cycle, and the  $E_{PE}$  includes switching and conduction loss. Details can be found in [37].

The design variables of the optimisation problem and their bounds are provided in Table 9. The constraints are defined as in Table 10, and the expressions are in Equations (24) and (25), respectively.

$$E_c \leq E_{batt} \tag{24}$$

$$N_{em}P_{in} \leq P_{batt} \tag{25}$$

where  $P_{in} = \sqrt{3}V_r I_{max}$  is the input power of the motor.  $V_r$  and  $I_{max}$  are the rated voltage and maximum current of the electric motor.

**Table 9.** Design variables for the EV optimisation problem.

Variables	Meaning	Lower Bound	Upper Bound	Unit
$N_{sc}$	Number of battery cells in series	4	8	
$N_{pc}$	Number of battery cells in parallel	80	84	
$N_{bc}$	Total number of battery cells	320	672	
$k_a$	Axial scaling ratio of motor	0.8	1.4	
$k_r$	Radial scaling ratio of motor	0.8	1.4	
$I_{rms}$	RMS current of motor	100	405	A
$V_r$	Rated voltage	210	230	V

**Table 10.** Constraints for the EV optimisation problem.

Constraints	Meaning
$g_1$	Energy consumption $\leq$ available energy in the battery pack
$g_2$	Motor input power $\leq$ battery output power

### 3.2. AiO Formulation

The AiO solved the whole problem together, as shown in Equation (26).

$$\begin{aligned} &\min (E_c, G_r) \\ &\mathbf{x} = [N_{sc}, N_{pc}, k_a, k_r, I_{rms}] \\ &s.t. \\ &E_c \leq E_{batt}, N_{em}P_{in} \leq P_{batt} \end{aligned} \tag{26}$$

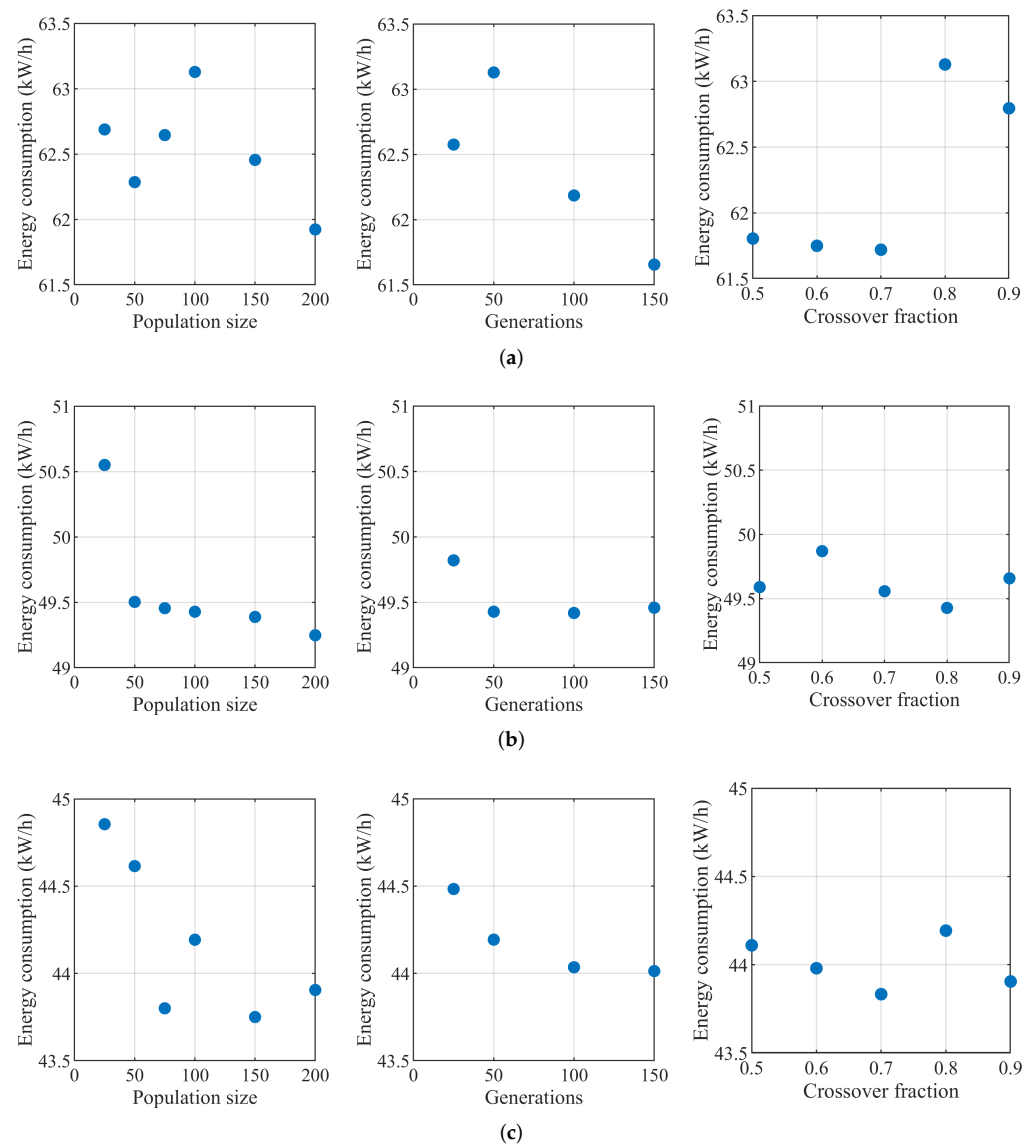
The number of battery cells in series  $N_{sc}$  and parallel  $N_{pc}$  can only be integers. Therefore, branch and bound (BnB) and genetic algorithm (GA) were applied since they could solve problems with integer design variables. In the BnB algorithm, the design variables were divided into smaller ranges (branches) within the lower and upper bounds in Table 9. For integer design variables, the bounds of each branch were integer values [38,39]. In this optimisation problem,  $G_r$  was converted into a design constraint and the objective function to be minimised was  $E_c$ . Each branch was optimised by the constraints method using an interior-point algorithm. The settings of the constraints method listed in Table 11 were selected for finding the best compromise between the accuracy and efficiency.

Similar to the BnB algorithm, the objective function  $G_r$  was converted into a constraint in the GA. The GA settings have to be selected considering both accuracy and efficiency. In order to select the proper settings, a sensitivity analysis on the population size, maximum number of generations, and crossover fraction was implemented [34,40].

**Table 11.** Settings of the constraints method used in AiO for the EV optimisation problem.

Options	Value
Algorithm	interior-point
Step Tolerance	$1 \times 10^{-10}$
Function Tolerance	$1 \times 10^{-6}$
Constraints Tolerance	$1 \times 10^{-6}$
Maximum number of function evaluations allowed	$3 \times 10^3$

The analysis was performed at three different levels of  $Gr$  as shown in Figure 12. A larger population size and higher number of generations would have helped to achieve more accurate results. However, they were expected to be as small as possible for higher efficiency as well. The crossover fraction was related to the crossover rate and mutation rate. A proper crossover fraction could help to reduce the number of generations. Moreover, it can be seen that, at different values of  $Gr$ , the influence of population size, maximum number of generations, and crossover fraction were not consistent. Therefore, the settings listed in Table 12 were selected based on a reasonable compromise between accuracy and efficiency.

**Figure 12.** Sensitivity analysis of GA settings. (a)  $1/Gr = 1.8$ , (b)  $1/Gr = 2.4$ , (c)  $1/Gr = 3.0$ .

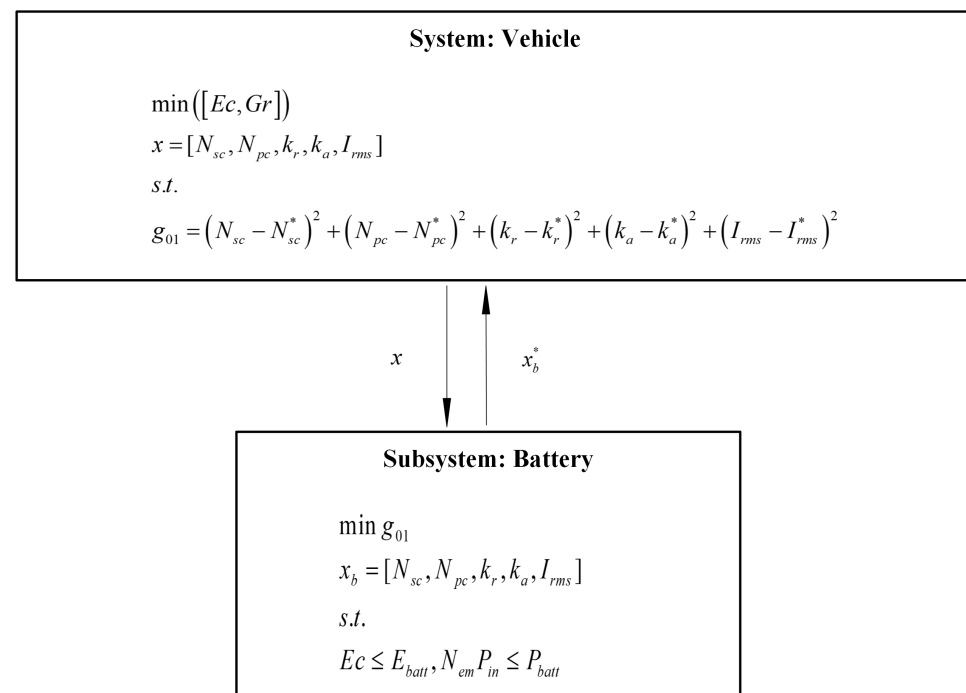
**Table 12.** Settings of GA for the EV optimisation problem.

Options	Value in AiO	Value in CO	Value in ATC
Population Size	150	150	100
Crossover Fraction	0.7	0.7	0.8
Function Tolerance	$1 \times 10^{-6}$	$1 \times 10^{-6}$	$1 \times 10^{-6}$
Constraint Tolerance	$1 \times 10^{-6}$	$1 \times 10^{-9}$	$1 \times 10^{-6}$
Maximum number of generations	150	200	50

### 3.3. CO Formulation

The formulation of the CO method is presented in Figure 13. The battery is a subsystem not included in the vehicle powertrain system level. The system level optimises all the objective functions considering all the design variables, as in the AiO formulation. The compatibility constraint  $g_{01}$  is applied at the system level.

The battery subsystem is connected with system level by linking variables, which are the design variables of the system level and subsystem level ( $x$  and  $x_b$ ). The objective of the subsystem is to minimise the discrepancy of the design variables between the system level and battery subsystem, subjected to the constraints  $g_1$  and  $g_2$  related to the battery energy and power. The expression of the objective function is the discrepancy between the target value of  $N_{bc}$  optimised at the system level and the product of  $N_{sc}$  and  $N_{pc}$  optimised at the subsystem level.

**Figure 13.** CO formulation for the EV optimisation problem.

Gradeability at the system level was converted to a constraint. Iteratively, a specific value of  $Gr$  was selected and the  $Ec$  was minimised, subject to the compatibility constraint. The optimal design variables  $x$  were then sent to the battery subsystem as the linking variables. The discrepancy between the system design variables  $x$  with respect to the subsystem design variables  $x_b$  was minimised in the battery subsystem. At the end of each iteration, the subsystem design variables  $x_b$  were sent back to the system level and used to compute the compatibility constraints  $g_{01}$ . The optimisation was terminated when the variation of  $Ec$  at the system level was small enough with respect to the previous



iteration. The convergence criterion was defined as the norm of the discrepancy between two iterations less than 0.005.

The GA settings were selected according to a sensitivity analysis performed above, listed in Table 12. This problem cannot be solved by the branch and bound algorithm due to the convergence issues.

### 3.4. ATC Formulation

In the ATC formulation, the problem was decomposed into vehicle performance design (system level) and battery design (subsystem level), as shown in Figure 14. The vehicle performance was optimised at the system level considering the objective functions  $Ec$  and  $Gr$ . The electric motor was also included in the system level. Therefore, the design variables of the system level were the total number of battery cells, the axial and radial electric motor scaling ratio and the rated voltage of the electric motor. The system level also acted as a coordinator sending the optimum value of  $N_{bc}$  to the battery subsystem as the design target. The constraints  $g_1$  and  $g_2$  are defined in Section 3.1.

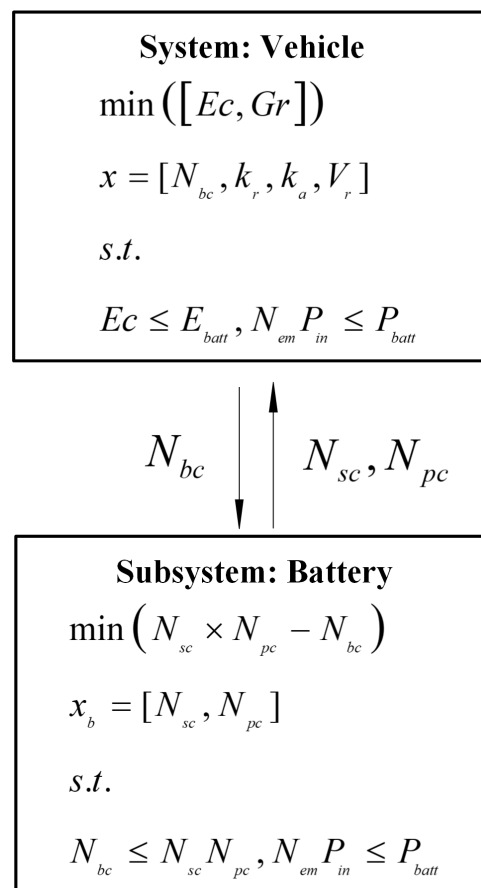


**Figure 14.** ATC formulation for the EV optimisation problem.

The battery subsystem has to reach the target value of  $N_{bc}$  by arranging the battery cells in the pack. Therefore, the design variables are  $N_{sc}$  and  $N_{pc}$ . The objective was evaluated by the discrepancy between the target value of  $N_{bc}$  and the product of the  $N_{sc}$  and  $N_{pc}$ . Moreover, one constraint was defined, as the total number of battery cells obtained in the subsystem (product of  $N_{sc}$  and  $N_{pc}$ ) should not be less than  $N_{bc}$ , defined at the system level, to ensure the available energy in the battery pack. Another constraint was  $g_2$ , in which the  $P_{in}$  was the shared variable from the system level.

The system level and subsystem level of the ATC formulation were optimised by two algorithms supporting integer design variables. The objective function  $Gr$  in the system level was converted into a constraint. The optimisation process is as follows. At the first

iteration, the system level is optimised and the target number of battery cells  $N_{bc}$  is sent to the battery subsystem. Then, the battery subsystem optimises the arrangement of cells in the battery pack, trying to minimise the discrepancy with the target  $N_{bc}$  from the system level. At the end of each iteration, the battery subsystem sends  $N_{sc}$  and  $N_{pc}$  back to the system level. The optimisation is terminated when the discrepancy between the target value of  $N_{bc}$  and the product of  $N_{sc}$  and  $N_{pc}$  in the current iteration is very close to the discrepancy at the last iteration. The convergence tolerance is set to 0.06.

Based on the sensitivity analysis, the settings of GA are listed in Table 12. The settings of the constraints method employed in the branch and bounds algorithm are the same as in the AiO formulation.

### 3.5. Solutions and Comparison of the MDO Methods

The optimal solutions for the powertrain optimisation problem obtained from the AiO, CO, and ATC methods are reported and analysed in this section. Since the problem includes integer design variables, the branch and bound algorithm, as well as the genetic algorithm, were applied to solve the individual optimisation problems. Gradeability  $Gr$  was converted into a constraint and energy consumption  $Ec$  was minimised. The range  $1/Gr$  in all the formulations was from 1.6 to 3.4. The Pareto-optimal sets from the proposed methods are compared in Figure 15. It can be seen that the energy consumption increases when higher gradeability is required.

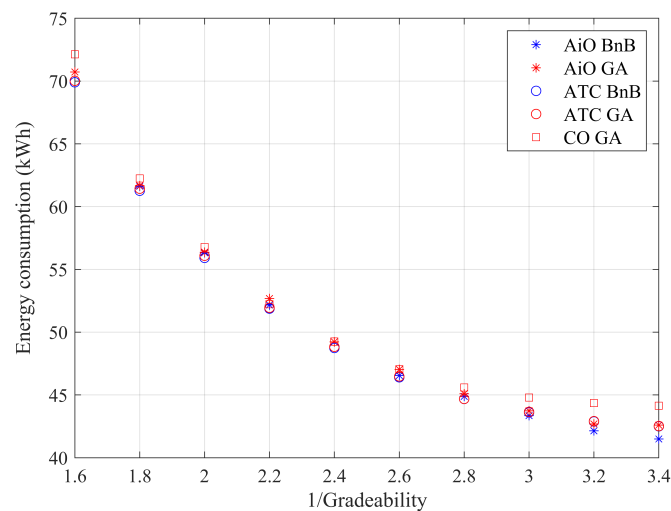


Figure 15. Pareto-optimal sets in the objective functions domain.

As for the suspension optimisation problem, a similar comparison of the three methods was performed referring to transparency, simplicity, efficiency, and accuracy. The AiO is the simplest formulation in terms of transparency and simplicity. The problem needs to be decomposed both in CO and ATC, while ATC is more complex to understand and implemented. Therefore, the ranking for transparency and simplicity is AiO, CO, and ATC.

The number of iterations and computational effort at different values of gradeability are related to the initial values of the design variables. Therefore, the efficiency was evaluated by the computational time reported in Table 13. It can be concluded that the ATC is more efficient than AiO when the same algorithm is employed. The efficiency of BnB algorithm is higher than GA in AiO and ATC, while it shows convergence problem in CO. The CO solved by GA has the lowest efficiency.

**Table 13.** Computational effort for the EV optimisation problem.

Formulation	Algorithm	Time (s)
AiO	Branch and bound	4851
AiO	Genetic algorithm	37,970
CO	Branch and bound	/
CO	Genetic algorithm	590,342
ATC	Branch and bound	1659
ATC	Genetic algorithm	28,213

The accuracy of the three methods was evaluated by comparing the results with a reference set of optimal solutions. A Sobol low discrepancy sequence was used for sampling the design variables within their bounds. The optimal values of objective functions were then sorted, including the constraints  $g_1$  and  $g_2$ . It is evident that AiO and ATC have similar accuracy, and both are better than CO.

#### 4. Conclusions

Optimisation problems in the vehicle design field were solved by MDO methods, namely AiO, CO, and ATC. The simplicity, transparency, accuracy, and efficiency of the methods were analysed and compared for the solution of the two problems. It turns out that AiO is the simplest formulation to understand and implement, with moderate accuracy and efficiency. ATC is the best choice for both problems, since it can efficiently provide solutions with good accuracy. However, the formulation and implementation cost of ATC is relevant. Similar to ATC, CO also needs special effort in the formulation and programming process. However, its accuracy and efficiency are not as good as ATC. It also should be noted that ATC convergence was proven by other researchers [12], but the CO might have convergence problem [18].

Both the considered suspension design and the EV powertrain design are typical multi-objective optimisation problems with many design variables, while they do cover different levels of complexity. Therefore, the results described in this paper can be considered quite general for most problems. The comparison of the considered MDO methods is summarised in Table 14. There is no method evaluated as poor in the table since other MDO methods, such as BLISS and CSSO, which may perform poorly, based on the studies in the literature, were excluded a priori. Independently from the MDO method applied, the optimisation algorithm and related settings need to be selected properly for the specific optimisation problem. The results described in the paper could help designers to apply MDO methods while optimising complex systems in the vehicle chassis development process.

**Table 14.** Comparison of MDO methods.

MDO Method	No. of Levels	Efficiency	Simplicity	Transparency	Accuracy
AiO	1	-	++	++	+
CO	2	-	+	+	-
ATC	$\geq 2$	++	-	-	+

Note: ++ very good, + good, - acceptable.

**Author Contributions:** Conceptualization, L.Y. and M.G.; methodology, M.G.; software, L.Y.; validation, G.M., G.P. and F.B.; writing—original draft preparation, L.Y.; writing—review and editing, M.G.; supervision, M.G. All authors have read and agreed to the published version of the manuscript.

**Institutional Review Board Statement:** Not applicable.

**Informed Consent Statement:** Not applicable.

**Data Availability Statement:** Not applicable.

**Conflicts of Interest:** The authors declare no conflict of interest.

## References

1. Ryberg, A.B. *Metamodel-Based Multidisciplinary Design Optimization of Automotive Structures*; Linköping University Electronic Press: Linköping, Sweden, 2017; Volume 1870.
2. Yang, L.; Ballo, F.; Previati, G.; Gobbi, M.; Mastinu, G. On the use of Multi-disciplinary optimisation methods for road vehicle passive suspension design. In Proceedings of the 21st International Conference on Advanced Vehicle Technologies, Anaheim, CA, USA, 18–21 August 2019.
3. Wang, G.G.; Shan, S. Review of metamodeling techniques in support of engineering design optimization. *J. Mech. Des.* **2007**, *129*, 370–380. [[CrossRef](#)]
4. Michelena, N.; Kim, H.M.; Papalambros, P. A system partitioning and optimization approach to target cascading. In Proceedings of the 12th International Conference on Engineering Design, Munich, Germany, 24–26 August 1999.
5. Kim, H.M.; Rideout, D.G.; Papalambros, P.Y.; Stein, J.L. Analytical target cascading in automotive vehicle design. *J. Mech. Des.* **2003**, *125*, 481–489. [[CrossRef](#)]
6. Kim, H.M.; Michelena, N.F.; Papalambros, P.Y.; Jiang, T. Target cascading in optimal system design. *J. Mech. Des.* **2003**, *125*, 474–480. [[CrossRef](#)]
7. Kokkolaras, M.; Louca, L.; Delagrammatikas, G.; Michelena, N.; Filipi, Z.; Papalambros, P.; Stein, J.; Assanis, D. Simulation-based optimal design of heavy trucks by model-based decomposition: An extensive analytical target cascading case study. *Int. J. Heavy Veh. Syst.* **2004**, *11*, 403–433. [[CrossRef](#)]
8. Kianifar, M.R.; Campean, I.F. Analytical target cascading framework for engine calibration optimisation. *Int. J. Powertrains* **2014**, *3*, 279–302. [[CrossRef](#)]
9. Bayrak, A.E.; Kang, N.; Papalambros, P.Y. Decomposition-based design optimization of hybrid electric powertrain architectures: Simultaneous configuration and sizing design. *J. Mech. Des.* **2016**, *138*, 071405. [[CrossRef](#)]
10. Blouin, V.; Fadel, G.; Haque, I.; Wagner, J.; Samuels, H. Continuously variable transmission design for optimum vehicle performance by analytical target cascading. *Int. J. Heavy Veh. Syst.* **2004**, *11*, 327–348. [[CrossRef](#)]
11. Gandikota, I.; Rais-Rohani, M.; DorMohammadi, S.; Kiani, M. Multilevel vehicle - dummy design optimization for mass and injury criteria minimization. *Proc. Inst. Mech. Eng. Part D J. Automob. Eng.* **2015**, *229*, 283–295. [[CrossRef](#)]
12. Michelena, N.; Park, H.; Papalambros, P.Y. Convergence properties of analytical target cascading. *AIAA J.* **2003**, *41*, 897–905. [[CrossRef](#)]
13. Braun, R.D. Collaborative Optimization: An Architecture for Large-Scale Distributed Design. Ph.D. Thesis, Stanford University, Stanford, CA, USA, 1996.
14. Braun, R.D.; Moore, A.A.; Kroo, I.M. Collaborative approach to launch vehicle design. *J. Spacecr. Rocket.* **1997**, *34*, 478–486. [[CrossRef](#)]
15. Wang, W.; Gao, F.; Cheng, Y.; Lin, C. Multidisciplinary design optimization for front structure of an electric car body-in-white based on improved collaborative optimization method. *Int. J. Automot. Technol.* **2017**, *18*, 1007–1015. [[CrossRef](#)]
16. Xue, Z.; Elango, A.; Fang, J. Multidisciplinary design optimization of vehicle weight reduction. *SAE Int. J. Mater. Manuf.* **2016**, *9*, 393–399. [[CrossRef](#)]
17. Allison, J.; Kokkolaras, M.; Zawislak, M.; Papalambros, P.Y. On the use of analytical target cascading and collaborative optimization for complex system design. In Proceedings of the 6th World Congress on Structural and Multidisciplinary Optimization, Rio de Janeiro, Brazil, 30 May–3 June 2005.
18. Balesdent, M.; Bérend, N.; Dépincé, P.; Chriette, A. A survey of multidisciplinary design optimization methods in launch vehicle design. *Struct. Multidiscip. Optim.* **2012**, *45*, 619–642. [[CrossRef](#)]
19. Azadi, M.; Azadi, S.; Zahedi, F.; Moradi, M. Multidisciplinary Optimization of a Car Component Under NVH and Weight Constraints Using RSM. *Int. J. Vehicle Noise Vib.* **2009**, *5*, 261–270. [[CrossRef](#)]
20. Driant, T.; Moreau, S.; Fellouah, H.; Desrochers, A. Aero-Thermal Optimization of a Hybrid Roadster Tricycle Using Multidisciplinary Design Optimization Tools. In Proceedings of the ASME 2014 4th Joint US-European Fluids Engineering Division Summer Meeting Collocated with the ASME 2014 12th International Conference on Nanochannels, Microchannels, and Minichannels, Chicago, IL, USA, 3–7 August 2014.
21. Tao, S.; Shintani, K.; Bostanabad, R.; Chan, Y.C.; Yang, G.; Meingast, H.; Chen, W. Enhanced Gaussian process metamodeling and collaborative optimization for vehicle suspension design optimization. In Proceedings of the VEXTEC Presenting at ASME 2017 International Design Engineering Technical Conferences, Cleveland, OH, USA, 6–9 August 2017.
22. Zhao, W.; Wang, Y.; Wang, C. Multidisciplinary optimization of electric-wheel vehicle integrated chassis system based on steady endurance performance. *J. Clean. Prod.* **2018**, *186*, 640–651. [[CrossRef](#)]
23. Mitschke, M.; Wallentowitz, H. *Dynamik der Kraftfahrzeuge*; Springer Fachmedien Wiesbaden: Wiesbaden, Germany, 2014. [[CrossRef](#)]
24. Crolla, D.; Foster, D.E.; Kobayashi, T.; Vaughan, N. (Eds.) *Encyclopedia of Automotive Engineering*; John Wiley & Sons, Ltd.: Chichester, UK, 2014. [[CrossRef](#)]
25. Mastinu, G.; Ploechl, M. *Road and Off-Road Vehicle System Dynamics Handbook*; CRC Press, Taylor & Francis Group: Boca Raton, FL, USA, 2014.
26. Guiggiani, M. *The Science of Vehicle Dynamics: Handling, Braking, and Ride of Road and Race Cars*; Springer Science & Business Media: Berlin/Heidelberg, Germany, 2014.

27. Abe, M. *Vehicle Handling Dynamics: Theory and Application*; Butterworth-Heinemann: Oxford, UK, 2015.
28. Rill, G. *Road Vehicle Dynamics, Fundamentals and Modeling*; CRC Press, Taylor & Francis Group: Boca Raton, FL, USA, 2012.
29. Pacejka, H. *Tyre and Vehicle Dynamics*, 3rd ed.; Butterworth-Heinemann: Oxford, UK, 2012.
30. Ramakrishnan, K.; Yang, L.; Ballo, F.M.; Gobbi, M.; Mastinu, G. Multi-objective optimization of road vehicle passive suspensions with inerter. In Proceedings of the ASME 2016 International Design Engineering Technical Conferences and Computers and Information in Engineering Conference, Charlotte, NC, USA, 21–24 August 2016.
31. Gobbi, M.; Mastinu, G. Analytical description and optimization of the dynamic behaviour of passively suspended road vehicles. *J. Sound Vib.* **2001**, *245*, 457–481. [[CrossRef](#)]
32. Guarneri, P.; Gobbi, M.; Papalambros, P. Multi-objective, multi-level design optimization of ground vehicle suspension design. In Proceedings of the 8th World Congress on Structural and Multidisciplinary Optimization, Lisbon, Portugal, 1–5 June 2009; pp. 1–5.
33. Yang, L. Optimal Design of Road Vehicles Subsystems. Ph.D. Thesis, Politecnico di Milano, Milan, Italy, 2019.
34. Mastinu, G.; Gobbi, M.; Miano, C. *Optimal Design of Complex Mechanical Systems: With Applications to Vehicle Engineering*; Springer Science & Business Media: Berlin/Heidelberg, Germany, 2007.
35. Perez, R.; Liu, H.; Behdinin, K. Evaluation of multidisciplinary optimization approaches for aircraft conceptual design. In Proceedings of the 10th AIAA/ISSMO Multidisciplinary Analysis and Optimization Conference, Albany, NY, USA, 30 August–1 September 2004.
36. Ramakrishnan, K.; Mastinu, G.; Gobbi, M. Multidisciplinary Design of Electric Vehicles Based on Hierarchical Multi-Objective Optimization. *J. Mech. Des.* **2019**, *141*, 091404. [[CrossRef](#)]
37. Ramakrishnan, K. Multidisciplinary Design of Electric Vehicles Based on Hierarchical Multi-Objective Optimization. Ph.D. Thesis, Politecnico di Milano, Milan, Italy, 2017.
38. Clausen, J. *Branch and Bound Algorithms-Principles and Examples*; Department of Computer Science, University of Copenhagen: Copenhagen, Denmark, 1999; pp. 1–30.
39. Venkataraman, P. *Applied Optimization with MATLAB Programming*; John Wiley & Sons: Chichester, UK, 2009.
40. Gobbi, M. A  $k$ ,  $k$ - $\epsilon$  optimality selection based multi objective genetic algorithm with applications to vehicle engineering. *Optim. Eng.* **2013**, *14*, 345–360. [[CrossRef](#)]